Turkish J. Eng. Env. Sci.
33 (2009) , 167 – 184.

doi:10.3906/muh-0905-6

Hall current and heat transfer effects on MHD flow in a channel partially filled with a porous medium in a rotating system

Dileep Singh CHAUHAN and Priyanka RASTOGI
Department of Mathematics, University of Rajasthan, Jaipur-302055, INDIA
e-mail: dileepschauhan@yahoo.com

Received 04.05.2009

Abstract

MHD viscous electrically conducting fluid flow and heat transfer in a parallel plate channel partially filled with a porous medium and partially with a clear fluid was considered in the presence of an inclined magnetic field in a rotating system. Hall effects were taken into account. It was found that the Coriolis force, Hall current, and the permeability of the porous medium influenced significantly the flow behavior in the channel and the temperature field. Effects of the rotation parameter (R), Hall current parameter (m), permeability of the porous material (K), viscosities ratio parameter (ϕ_1), Hartmann number (M), and angle of inclination (θ) of the applied magnetic field (H_0) on the velocity distributions, temperature distributions, and the rate of heat transfer are depicted graphically and discussed.

Key Words: Hall current, Heat transfer, Permeability, Rotating system, Porous medium.

Introduction

The study of heat transfer processes in porous media is a well developed field of investigation because of its importance in a variety of situations occurring in geothermal systems, microelectronic heat transfer equipment, thermal insulation, and thermoacoustic engines, which can provide cooling or heating using environmentally benign gases as the working fluid. Nield and Bejan (2006) surveyed in detail this topic. In recent years, studies of heat transfer and flow of electrically conducting viscous fluids through a porous medium have attracted considerable attention, in the presence of a magnetic field, e.g. Bian et al. (1996), McWhirter et al. (1998a, 1998b), Geindreau and Auriault (2002), Seddeek (2002), Chauhan and Jain (2005), Hayat et al. (2007a, 2008), and Sunil and Mahajan (2009).

The study of the interaction of the Coriolis force with the electromagnetic force is important. In particular, rotating MHD flows in porous media with heat transfer is one of the important current topics because of its applications in thermofluid transport modeling in magnetic geosystems (Armstead, 1982), meteorology, MHD power generators, turbo machinery, solidification process in metallurgy, and in some astrophysical problems. It is generally thought that the existence of the geomagnetic field is due to finite amplitude instability of the Earth's core. Since most cosmic bodies are rotators, the study of convective motions in a rotating electrically

conducting fluid is essential in understanding better the magnetohydrodynamics of the interiors of the Earth and other planets. It has motivated a number of studies on convective motions in hydromagnetic rotating systems, which can provide explanations for the observed variations in the geomagnetic field. The rotating flow subjected to different physical effects has been studied by many authors, such as Eltayeb and Roberts (1970), Childress and Soward (1972), Eltayeb (1972), Singh et al. (1994), Nield (1999), Riahi (2002), Krishna et al.(2002), Bég et al. (2008), and Seth et al. (2009).

In most cases, the Hall term is ignored in applying Ohm's law as it has no marked effect for small magnetic fields. However, to study the effects of strong magnetic fields on the electrically conducting fluid flow, we see that the influence of the electromagnetic force is noticeable and causes anisotropic electrical conductivity in the plasma. This anisotropy in the electrical conductivity of the plasma produces a current known as the Hall current. The Hall effect is important when the magnetic field is high or when the collision frequency is low, causing the Hall parameter to be significant (Sutton and Sherman, 1965). The effects of Hall current on the fluid flow and heat transfer in rotating channels have many engineering applications in flows of laboratory plasmas, in MHD power generation, in MHD accelerators, and in several astrophysical and geophysical situations. Thus, in a rotating system, the effect of Hall current on MHD flow in parallel plate channels has been investigated by many researchers. Mandal and Mandal (1983) and Ghosh (2002) investigated effects of Hall current on MHD Couette flow between parallel plates in a rotating system. Raghavachar and Gothandaraman (1989) studied hydromagnetic convection in a rotating fluid layer in the presence of Hall current. Ghosh and Bhattacharjee (2000) considered Hall effects on MHD flow in a rotating channel in the presence of an inclined magnetic field. Hayat et al. (2005) investigated the effects of Hall current on unsteady flow of a non-Newtonian fluid in a rotating system. Recently, Ghosh et al. (2009) investigated Hall effects on heat transfer and MHD flow in a rotating channel.

The flow of fluids through and across a porous medium is a topic of special interest in many engineering challenges, for example, in the chemical industry separation processes, in pollutant dispersion along aquifers, and in environmental transport processes in soils (Bear and Bachmat, 1987). The effects of Hall current were investigated by Hayat et al. (2007b, 2007c) on the rotating oscillating flows of non-Newtonian fluids through porous medium. Bég et al. (2008) studied the transient viscous incompressible hydrodynamic Couette flow in a rotating porous medium. Flow in channels partially filled by a porous medium and partially filled by a clear fluid is important because such fluid flow situations occur in many engineering applications. Coupled and heat transfer problems in channels partially filled by a porous medium were studied analytically by Kim and Russell (1985), Chauhan and Gupta (1999), Kuznetsov (1996, 1998, 2000), Al-Nimr and Khadrawi (2003), and many others.

The present study investigates the magnetohydrodynamic flow of an electrically conducting fluid with heat transfer in a parallel plate channel partially filled by a porous medium. Channel is rotating with uniform angular velocity Ω about an axis normal to the plates. A uniform magnetic field H_0 is applied at an angle θ from the positive direction of axis of rotation. The Hall effects are taken into consideration. Exact analytic solutions are provided, by taking appropriate boundary conditions. In solving this problem, we utilize the boundary conditions at the clear fluid-porous medium interface, suggested by Ochao-Tapia and Whitaker (1995a, 1995b). The physical interpretation for the various parameters is discussed with the help of graphs.

Formulation of the problem

The steady flow of a viscous incompressible electrically conducting fluid in an infinite parallel plate channel partially filled with a porous medium and rotating with uniform angular velocity Ω about an axis normal to the plates is considered. A uniform magnetic field H_0 inclined at an angle θ from the positive direction of the axis of rotation is applied. A porous material of thickness 'h' is fixed to the lower impermeable plate, which is maintained at a constant temperature T_0, and the upper impermeable plate is fixed at a distance 'L' from the porous interface and maintained at a constant temperature T_1. A Cartesian coordinate system is taken with x and y axis lying on the porous-clear fluid interface and z axis perpendicular to it (see Figure 1). A constant pressure gradient $\left(-\frac{\partial p}{\partial x}\right)$ is applied at the mouth of the channel to generate the primary flow in the x-direction. Secondary flow is induced in the y-direction due to rotation/Hall effect and $\frac{\partial p}{\partial y}$ is taken as zero. In the case of a strong applied magnetic field, the Hall effect induces an electric current that flow normally to both the magnetic and electric field, which in turn induces a transverse motion of the fluid. Thus Hall current induces a secondary flow, and so there will be 2 components of the velocity. All physical quantities are assumed to be functions of z only, since the channel is infinite along the x and y directions. The flow and temperature field is divided into 2 regions:

I-Region ($0 \leq z \leq L$), clear fluid region; and

II-Region ($-h \leq z \leq 0$), porous region.

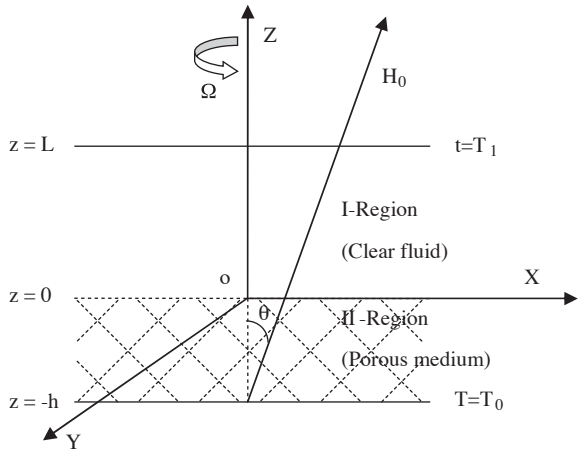

Figure 1. Schematic diagram.

For this physical situation, we assume the velocity vector q, magnetic field H, electric field E, current density vector J in clear fluid region (I-region), and $\bar{q},\ \bar{H}, \bar{E},\ \bar{J}$ in the porous region (II-region) as follows:

$$q = (u',\ v',\ 0); \quad \bar{q} = (U',\ V',\ 0)$$

$$H = (h_1' + H_0 \sin\theta,\ h_2',\ H_0 \cos\theta); \quad \bar{H} = (H_1' + H_0 \sin\theta,\ H_2',\ H_0 \cos\theta)$$

$$E = (E_1',\ E_2',\ E_3'); \quad \bar{E} = (\bar{E}_1',\ \bar{E}_2',\ \bar{E}_3')$$

$$J = (J_1',\ J_2',\ 0); \quad \bar{J} = (\bar{J}_1',\ \bar{J}_2',\ 0) \tag{1}$$

and t', T' are the temperatures in the clear fluid region and porous medium respectively.

The governing MHD equations in a rotating frame of reference for flow, magnetic field, and temperature distribution in the 2 regions are given by

For region-I (clear fluid region)

$$\frac{\partial u'}{\partial x} + \frac{\partial v'}{\partial y} = 0, \tag{2}$$

$$-2\Omega v' = \upsilon \frac{\partial^2 u'}{\partial z^2} + \frac{\mu_e}{\rho} J_2 H_0 \cos\theta - \frac{1}{\rho}\frac{\partial p}{\partial x}, \tag{3}$$

$$2\Omega u' = \upsilon \frac{\partial^2 v'}{\partial z^2} - \frac{\mu_e}{\rho} J_1 H_0 \cos\theta, \tag{4}$$

$$0 = \frac{k}{\rho C_p}\frac{\partial^2 t'}{\partial z^2} + \frac{\upsilon}{C_p}\left[\left(\frac{\partial u'}{\partial z}\right)^2 + \left(\frac{\partial v'}{\partial z}\right)^2\right] + \frac{1}{\sigma\ \rho C_p}\left[\left(\frac{\partial h_1'}{\partial z}\right)^2 + \left(\frac{\partial h_2'}{\partial z}\right)^2\right]. \tag{5}$$

For steady motion, the Maxwell equations and the generalized Ohm's law (Cowling, 1957), neglecting ion-slip and thermo-electric effect, are given by

$$\nabla \cdot B = 0, \tag{6}$$

$$\nabla \times E = 0, \tag{7}$$

$$\nabla \times H = J, \tag{8}$$

$$\nabla \cdot\ J = 0, \tag{9}$$

and

$$J + \frac{\tau_e \omega_e}{H_0}(J \times H) = \sigma\left[E + \mu_e (q \times H) + \frac{1}{e\eta_e}\nabla p_e\right], \tag{10}$$

where $B = \mu_e H$is the magnetic induction.

Here, $\rho,\ \mu_e,\ \upsilon,\ \sigma,\ \omega_e,\ \tau_e,\ e, \eta_e,\ p_e,\ k\ and\ C_p$are the fluid density, magnetic permeability, kinematic viscosity, electrical conductivity, cyclotron frequency, electron collision time, electric charge, number density of electron, electron pressure, thermal conductivity and specific heat at constant pressure.

For partially ionized gases, electron pressure gradient may be neglected, and it is also assumed that$\omega_i \tau_i << 1$, where ω_i and τ_i are the cyclotron frequency and the collision time of ions respectively.

Since all physical quantities are functions of z only, by Eq. (1), Eqs. (2), (6), and (9) are satisfied identically; and using Eqs. (7) and (8), Eqs. (3), (4), and (10) reduce to

$$\upsilon \frac{d^2 u'}{dz^2} + \frac{\mu_e}{\rho} H_0 \cos\theta \frac{dh_1'}{dz} + 2\Omega v' = \frac{1}{\rho}\frac{dp}{dx}, \tag{11}$$

$$\upsilon \frac{d^2 v'}{dz^2} + \frac{\mu_e}{\rho} H_0 \cos\theta \frac{dh_2'}{dz} - 2\Omega u' = 0, \tag{12}$$

$$\frac{d^2 h_2'}{dz^2} - m\cos\theta \frac{d^2 h_1'}{dz^2} + \sigma\ \mu_e H_0 \cos\theta \frac{dv'}{dz} = 0, \tag{13}$$

$$\text{and, } \frac{d^2 h_1'}{dz^2} + m\cos\theta \frac{d^2 h_2'}{dz^2} + \sigma\ \mu_e H_0 \cos\theta \frac{du'}{dz} = 0, \tag{14}$$

where $m = \tau_e \omega_e$ is the Hall current parameter.

Governing equations for region-II (porous region):

$$\frac{\partial U'}{\partial x} + \frac{\partial V'}{\partial y} = 0, \tag{15}$$

$$-2\Omega V' = \phi_1 \upsilon \frac{\partial^2 U'}{\partial z^2} + \frac{\mu_e}{\rho} \bar{J}_2 H_0 \cos\theta - \frac{\upsilon}{K_0} U' - \frac{1}{\rho}\frac{\partial p}{\partial x}, \tag{16}$$

$$2\Omega U' = \phi_1 \upsilon \frac{\partial^2 V'}{\partial z^2} - \frac{\mu_e}{\rho} \bar{J}_1 H_0 \cos\theta - \frac{\upsilon}{K_0} V', \tag{17}$$

$$\begin{aligned} 0 = \; & \tfrac{\bar{k}}{\rho C_p}\tfrac{\partial^2 T'}{\partial z^2} + \tfrac{\mu}{K_0 \rho C_p}\left(U'^2 + V'^2\right) + \tfrac{\overline{\mu}}{\rho C_p}\left[\left(\tfrac{\partial U'}{\partial z}\right)^2 + \left(\tfrac{\partial V'}{\partial z}\right)^2\right] \\ & + \tfrac{1}{\sigma\ \rho C_p}\left[\left(\tfrac{\partial H_1'}{\partial z}\right)^2 + \left(\tfrac{\partial H_2'}{\partial z}\right)^2\right], \end{aligned} \tag{18}$$

where $\phi_1 = \frac{\overline{\mu}}{\mu}$; μ, the clear fluid viscosity; $\overline{\mu}$, the effective viscosity of the fluid in porous medium; K_0, the permeability of the porous medium; and $\overline{k}$, the effective thermal conductivity in the porous medium.

For steady motion, the Maxwell equations and Ohm's law, taking Hall current into account, are given by

$$\nabla \cdot \overline{B} = 0, \tag{19}$$

$$\nabla \times \overline{E} = 0, \tag{20}$$

$$\nabla \times \overline{H} = \overline{J}, \tag{21}$$

$$\nabla \cdot \overline{J} = 0, \tag{22}$$

$$\text{and, } \overline{J} + \frac{\tau_e \omega_e}{H_0}\left(\overline{J} \times \overline{H}\right) = \sigma\left[\overline{E} + \mu_e\left(\bar{q} \times \overline{H}\right) + \frac{1}{e\eta_e}\nabla p_e\right], \tag{23}$$

where $\overline{B} = \mu_e \overline{H}$.

Since all physical quantities are functions of z only, using Eq. (1), Eqs. (15), (19), and (22) are satisfied identically; using Eqs. (20) and (21), Eqs. (16), (17), and (23) reduce to

$$\phi_1 \upsilon \frac{d^2 U'}{dz^2} + \frac{\mu_e}{\rho} H_0 \cos\theta \frac{dH_1'}{dz} - \frac{\upsilon}{K_0} U' + 2\Omega V' = \frac{1}{\rho}\frac{dp}{dx}, \tag{24}$$

$$\phi_1 \upsilon \frac{d^2 V'}{dz^2} + \frac{\mu_e}{\rho} H_0 \cos\theta \frac{dH_2'}{dz} - \frac{\upsilon}{K_0} V' - 2\Omega U' = 0, \tag{25}$$

$$\frac{d^2 H_2'}{dz^2} - m\cos\theta \frac{d^2 H_1'}{dz^2} + \sigma\ \mu_e H_0 \cos\theta \frac{dV'}{dz} = 0, \tag{26}$$

$$\text{and, } \frac{d^2 H_1'}{dz^2} + m\cos\theta \frac{d^2 H_2'}{dz^2} + \sigma\ \mu_e H_0 \cos\theta \frac{dU'}{dz} = 0. \tag{27}$$

The corresponding boundary conditions are giv en by

$$
\begin{aligned}
&\text{at} \qquad z = L; u' = 0, v' = 0, h_1' = 0, h_2' = 0, t' = T_1,\\
&\text{at} \qquad z = 0; u' = U', v' = V', h_1' = H_1', h_2' = H_2', t' = T',\\
&\qquad \overline{\mu}\frac{dU'}{dz} - \mu\frac{du'}{dz} = \frac{\beta}{\sqrt{K_0}}\mu U', \quad \overline{\mu}\frac{dV'}{dz} - \mu\frac{dv'}{dz} = \frac{\beta}{\sqrt{K_0}}\mu V',\\
&\qquad \frac{dh_1'}{dz} = \frac{dH_1'}{dz}, \quad \frac{dh_2'}{dz} = \frac{dH_2'}{dz}, \quad k\frac{dt'}{dz} = \overline{k}\frac{dT'}{dz},\\
&\text{at} \qquad z = -h; U' = 0, V' = 0, H_1' = 0, H_2' = 0, t' = T_0,
\end{aligned} \tag{28}
$$

where β is a constant.

Solutions of the problem

We introduce the following non-dimensional quantities:

$$
\begin{aligned}
&\eta = \tfrac{z}{L}, \quad u = \tfrac{L}{\upsilon}u', \quad v = \tfrac{L}{\upsilon}v', \quad h_1 = \tfrac{1}{\sigma\ \mu_e \upsilon H_0}h_1', \quad h_2 = \tfrac{1}{\sigma\ \mu_e \upsilon H_0}h_2',\\
&K = \tfrac{K_0}{L^2}, U = \tfrac{L}{\upsilon}U', V = \tfrac{L}{\upsilon}V', \quad H_1 = \tfrac{1}{\sigma\ \mu_e \upsilon H_0}H_1', \quad H_2 = \tfrac{1}{\sigma\ \mu_e \upsilon H_0}H_2', t = \tfrac{t'-T_0}{T_1-T_0}, \quad T = \tfrac{T'-T_0}{T_1-T_0}.
\end{aligned} \tag{29}
$$

Using above non-dimensional quantities, and the following new complex variables,

$$
\begin{aligned}
F = u + iv \quad , \quad H = h_1 + ih_2,\\
\overline{F} = U + iV, \quad \overline{H} = H_1 + iH_2,
\end{aligned} \tag{30}
$$

Eqs. (11-14), (24-27), and Eqs. (5) and (18) reduce to

$$\frac{d^2F}{d\eta^2} + M^2\cos\theta\frac{dH}{d\eta} - 2iRF = -G, \tag{31}$$

$$(1 - im\cos\theta)\frac{d^2H}{d\eta^2} + \cos\theta\frac{dF}{d\eta} = 0, \tag{32}$$

$$\frac{d^2\overline{F}}{d\eta^2} + \frac{M^2\cos\theta}{\phi_1}\frac{d\overline{H}}{d\eta} - K_1\overline{F} - \frac{2iR\overline{F}}{\phi_1} = -\frac{G}{\phi_1}, \tag{33}$$

$$(1 - im\cos\theta)\frac{d^2\overline{H}}{d\eta^2} + \cos\theta\frac{d\overline{F}}{d\eta} = 0, \tag{34}$$

$$\frac{d^2t}{d\eta^2} + \Pr Ec\left[\left(\frac{dF}{d\eta}\right)\left(\frac{dF}{d\eta}\right)^c + M^2\left(\frac{dH}{d\eta}\right)\left(\frac{dH}{d\eta}\right)^c\right] = 0, \tag{35}$$

$$\frac{d^2T}{d\eta^2} + \frac{\Pr Ec}{\phi_2}\left[\frac{1}{K}\left(\overline{F}\ \overline{F}^c\right) + \phi_1\left(\frac{d\overline{F}}{d\eta}\right)\left(\frac{d\overline{F}}{d\eta}\right)^c + M^2\left(\frac{d\overline{H}}{d\eta}\right)\left(\frac{d\overline{H}}{d\eta}\right)^c\right] = 0, \tag{36}$$

where the superscript c denotes the complex conjugate, and $K_1 = \frac{1}{K\phi_1}$, $M = \mu_e H_0 L\sqrt{\frac{\sigma}{\rho\upsilon}}$, the Hartmann number, $R = \frac{\Omega L^2}{\upsilon}$, the rotation parameter, $G = \frac{L^3}{\rho\upsilon^2}\left(-\frac{\partial p}{\partial x}\right)$, the non-dimensional pressure gradient, $Ec = \frac{\upsilon^2}{L^2 C_p(T_1-T_0)}$, the Eckart number, and $\Pr = \frac{\upsilon\rho C_p}{k}$ is the Prandtl number.

The corresponding boundary conditions in non-dimensional form are given by

$$\begin{aligned}
&\text{at} \quad \eta = 1; F = 0, H = 0, t = 1,\\
&\text{at} \quad \eta = 0; F = \bar{F}, H = \bar{H}, t = T,\\
&\phi_1\frac{d\bar{F}}{d\eta} - \frac{dF}{d\eta} = \frac{\beta}{\sqrt{K}}\bar{F}, \quad \frac{dH}{d\eta} = \frac{d\bar{H}}{d\eta}, \quad \frac{dt}{d\eta} = \phi_2\frac{dT}{d\eta},\\
&\text{at} \quad \eta = -\alpha; \bar{F} = 0, \bar{H} = 0, T = 0.
\end{aligned} \tag{37}$$

where $\alpha = \frac{h}{L}$, and $\phi_2 = \frac{\overline{k}}{k}$.

Integrating Eq. (32), we obtain

$$\frac{dH}{d\eta} = -\frac{(A_1 + F\cos\theta)}{(1 - im\cos\theta)}, \tag{38}$$

where $A_1$is a constant of integration.

Using Eq. (38) in Eq. (31), we get

$$\frac{d^2F}{d\eta^2} - A^2F = A_1B - G, \tag{39}$$

where $A^2 = \frac{M^2\cos^2\theta}{1-im\cos\theta} + 2iR$,and $B = \frac{M^2\cos\theta}{1-im\cos\theta}$.

On solving Eq. (39), we obtain

$$F = A_2\sinh A\eta + A_3\cosh A\eta + \frac{G - BA_1}{A^2}, \tag{40}$$

Using (40) in (38), we get

$$\frac{dH}{d\eta} + A_1D + \frac{B}{M^2}\left\{\left(\frac{G - BA_1}{A^2}\right) + A_2\sinh A\eta + A_3\cosh A\eta\right\} = 0, \tag{41}$$

where $D = \frac{1}{1-im\cos\theta}$.

On solving (41), we obtain

$$H = -\left[A_1D\eta + \frac{B}{M^2}\left\{\left(\frac{G - BA_1}{A^2}\right)\eta + \frac{A_2\cosh A\eta + A_3\sinh A\eta}{A}\right\} + A_4\right]. \tag{42}$$

Similarly, we obtain the solution for the porous region:

$$\overline{F} = B_2\sinh C\eta + B_3\cosh C\eta + \frac{G - BB_1}{\phi_1 C^2}, \tag{43}$$

$$\overline{H} = -\left[B_1 D\eta + \frac{B}{M^2}\left\{\left(\frac{G - BB_1}{\phi_1 C^2}\right)\eta + \frac{B_2\cosh C\eta + B_3\sinh C\eta}{C}\right\} + B_4\right]. \tag{44}$$

Using the expressions of $F, H, \bar{F}, \bar{H}$ from Eqs. (40), (42-44) in Eqs. (35-36), and solving, we obtain the solutions for temperature fields in both regions:

$$\begin{aligned} t = \; & -\Pr Ec\left[\tfrac{F_1}{4a_3^2}\cosh 2a_3\eta - \tfrac{F_2}{4a_4^2}\cos 2a_4\eta + \tfrac{F_7}{4a_3^2}\sinh 2a_3\eta - \tfrac{F_8}{4a_4^2}\sin 2a_4\eta\right. \\ & + F_{14}\sinh a_3\eta\cos a_4\eta + F_{15}\cosh a_3\eta\sin a_4\eta + F_{16}\cosh a_3\eta\cos a_4\eta \\ & \left. + F_{17}\sinh a_3\eta\sin a_4\eta + \tfrac{F_9}{2}\eta^2\right] - (E_1\eta + E_2), \end{aligned} \tag{45}$$

$$\begin{aligned} T = \; & -\Pr Ec\left[\tfrac{F_{18}}{4c_3^2}\cosh 2c_3\eta - \tfrac{F_{19}}{4c_4^2}\cos 2c_4\eta + \tfrac{F_{24}}{4c_3^2}\sinh 2c_3\eta - \tfrac{F_{25}}{4c_4^2}\sin 2c_4\eta\right. \\ & + F_{31}\sinh c_3\eta\cos c_4\eta + F_{32}\cosh c_3\eta\sin c_4\eta + F_{33}\cosh c_3\eta\cos c_4\eta \\ & \left. + F_{34}\sinh c_3\eta\sin c_4\eta + \tfrac{F_{26}}{2}\eta^2\right] - (E_3\eta + E_4), \end{aligned} \tag{46}$$

where $A_1,\ A_2,\ A_3,\ A_4, B_1,\ B_2,\ B_3,\ B_4, E_1,\ E_2,\ E_3,\ E_4$ are constants of integration. These are obtained using the corresponding boundary conditions and reported in the appendix.

Rate of heat transfer at the upper plate

$$\begin{aligned} \left(\tfrac{dt}{d\eta}\right)_{\eta=1} = \; & -\Pr Ec\left[\tfrac{F_1}{2a_3}\sinh 2a_3 + \tfrac{F_2}{2a_4}\sin 2a_4 + \tfrac{F_7}{2a_3}\cosh 2a_3 - \tfrac{F_8}{2a_4}\cos 2a_4\right. \\ & + F_{10}\sinh a_3\cos a_4 + F_{11}\cosh a_3\sin a_4 + F_{12}\cosh a_3\cos a_4 \\ & \left. + F_{13}\sinh a_3\sin a_4 + F_9\right] - E_1. \end{aligned} \tag{47}$$

Rate of heat transfer at the porous medium interface

$$\left(\frac{dt}{d\eta}\right)_{\eta=0} = -\Pr Ec\left[\frac{F_7}{2a_3} - \frac{F_8}{2a_4} + F_{12}\right] - E_1. \tag{48}$$

Discussion

This study investigates the influence of Hall current and heat transfer effects on the rotating MHD flow in a channel partially filled by a porous medium. In this research we have taken the form of boundary conditions at the clear fluid-porous medium interface suggested by Ochao-Tapia and Whitaker (1995a, 1995b), who carried out a volume averaging analysis for the fluid-porous interface region. They have shown that the process of matching the Stokes' equations to the Brinkman-extended Darcy equation at the interface requires the continuity of velocity but a discontinuity in the shear stress. This condition for the jump in the shear stress includes an adjustable parameter, β, which allows necessary flexibility in modeling the porous interface region, and also to fit experimental data in the analytical results. When the parameter β is set equal to zero, the results reduce to the Brinkman model with the boundary condition as continuity of tangential shear stress at the porous interface. Ochao-Tapia and Whitaker (1995a, 1995b) provided the values of the parameter β for a

list of porous materials. We have utilized these values in this research and also compared these results with the case when $\beta = 0$.

The non-dimensional velocity components u and U in primary flow direction are plotted in Figures 2 and 3, for various values of the parameters K, R, m, β, θ and ϕ_1. The permeability K is a measure of the ease with which a fluid will flow through the porous medium; so for a given pressure gradient, Figure 2 shows that by increasing the permeability K of the porous medium, the primary velocity increases in the porous region and near its surface. However, it is reduced in the remaining channel and near the upper plate the effect of K is insignificant. The effects of other parameters can be seen in Figure 3. It is evident from this figure that the primary velocity in the channel decreases with the increase in the rotation parameter R in both clear fluid and porous medium region. It is observed that a maximum peak occurs in the middle of the composite channel when $R = 2$, which flattens as R is increased. The rotation parameter $R = \frac{\Omega L^2}{\upsilon}$ defines the relative magnitude of the Coriolis force and the viscous force in the regime; therefore it is clear that high magnitude Coriolis forces are counter-productive for the primary flow. The effect of β is to increase the primary flow inside the porous region and near its interface but it decreases in the middle and above. Further it is found that Hall parameter m decelerates the primary flow. It is seen that when the rotation is small, $R = 2$ by increasing the viscosities ratio parameter ϕ_1, primary flow velocity decreases because the effective viscosity of the fluid increases in the porous medium. However, when rotation is increased to $R = 9$, we observe that it increases in the channel except inside the porous medium and the nearby region of its interface. When the angle of inclination θ of the applied magnetic field with the positive direction of the axis of rotation is zero, the applied magnetic field becomes normal to the plates and as expected, by decreasing θ primary flow velocity decreases when rotation is small, $R = 2$. However, the results are more complex when rotation is large.

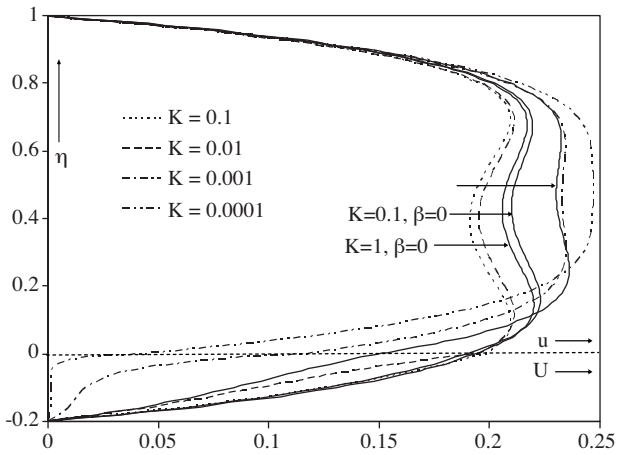

Figure 2. Primary velocity profiles u, U vs. η for G = 10, m = 1, $M^2 = 20$, R = 9, $\beta = 0.7$, $\phi_1 = 1.25$, $\theta = 45$.

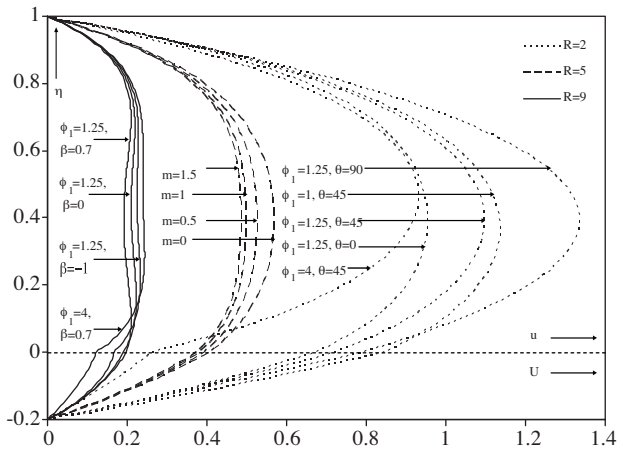

Figure 3. Primary velocity profiles u, U vs. η for G = 10, K = 0.1, m = 1, $M^2 = 20$,$\beta = 0.7$, $\phi_1 = 1.25$, $\theta = 45$.

The non-dimensional velocity components v and V in the secondary flow direction are plotted in Figures 4 and 5. It is found that the secondary flow velocity increases in magnitude with the increase in Hall parameter m. As reported in numerous MHD studies, this velocity component is a result of the Hall effect; therefore it will respond positively to increases in m values. It is also seen that the secondary flow is increased throughout the composite channel by increasing the permeability parameter K or angle of inclination θ or the parameter β, whereas it is decreased by increasing the viscosities ratio parameter ϕ_1. Further it is found that by increasing

the rotation parameter R, secondary flow becomes oscillatory.

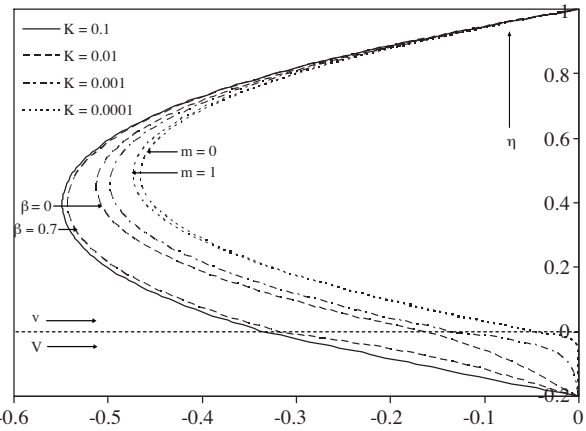

Figure 4. Secondary velocity profiles v, V vs. η for G = 10, m = 1, $M^2 = 20$, R = 9, $\beta = 0.7$, $\phi_1 = 1.25$, $\theta = 45$.

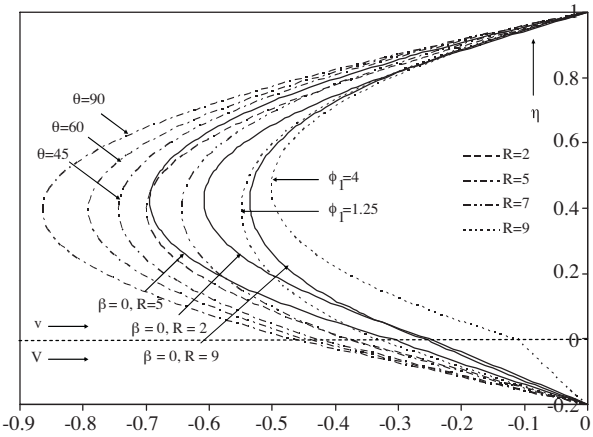

Figure 5. Secondary velocity profiles v, V vs. η for G = 10, K = 0.1, m = 1, $M^2 = 20$, $\beta = 0.7$, $\phi_1 = 1.25$, $\theta = 45$.

A similar trend is reported for the primary and secondary flows in a rotating parallel plates channel without porous substrate by Ghosh and Bhattacharjee (2000), Ghosh (2002), and Seth et al. (2009).

Figures 6 and 7 show the variation in induced magnetic field h_1, H_1 in primary flow direction and h_2, H_2 in secondary flow direction, respectively, for various values of the parameters. It is evident from these figures that these magnetic field components change sign in the composite channel. It is found in Figure 6 that the magnitude of induced magnetic field in primary flow direction is decreased by increasing the rotation parameter R. It is also decreased in the lower half channel by increasing β, but in the upper half it increases in magnitude. The permeability K of the porous medium also has the same effect on it as that of β. However, it is increased if we take Hall current into account $m = 1$, comparing to $m = 0$ case. Figure 7 shows that with the increase in the Hall current parameter m the magnitude of induced magnetic field in secondary flow direction decreases. When rotation is small, $R = 2$, it changes sign frequently in the channel and its magnitude increases with increasing R. However, by increasing β or K it increases in the upper half channel and decreases in magnitude in the lower half channel.

With the assumed boundary conditions, the equation of energy for the steady fully developed state has a solution that is independent of x and y. All the convective terms on the left-hand side become equal to zero. The resulting temperature distribution is, therefore, due to the generation of heat through viscous and joule dissipation, and to conduction in the transverse direction. In this case, that is when there is no convection of heat, the temperature distribution is seen to depend on the product $\Pr Ec = NBr$(Brinkman number) and M (Hartmann number).

Note that, for a given value of the temperature difference of the 2 walls of the channel$T_1 - T_0 > 0$, heat flows from the upper wall to the fluid, and as flow in the channel increases because of pressure gradient or other flow parameters, a reversal of the direction of the flow of heat at the upper plate occurs when the temperature gradient at it changes sign. For a given pressure gradient, we find critical Brinkman number$NBr^*(= \Pr Ec)$for which $\frac{dt}{d\eta} = 0$ at the upper wall. This critical Brinkman number indicates that heat flows from upper wall to fluid($NBr < NBr^*$), or heat flows from fluid to the upper wall($NBr > NBr^*$). This effect of heat transfer is of fundamental importance for the consideration of cooling at high velocities.

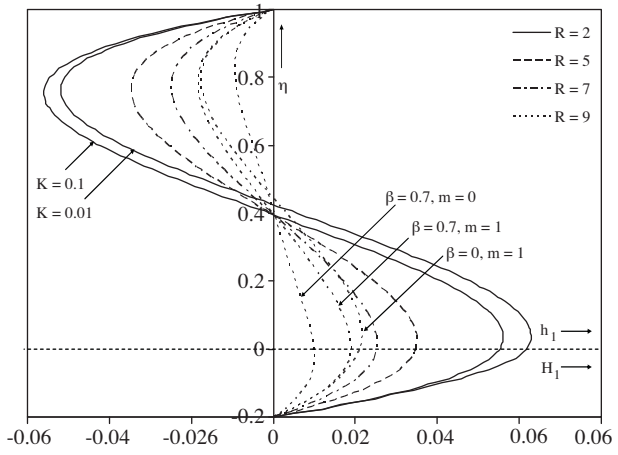

Figure 6. Induced magnetic field h_1, H_1 vs. η for G = 10, K = 0.1, m = 1, $M^2 = 20$, $\beta = 0.7$, $\phi_1 = 1.25$, $\theta = 45$.

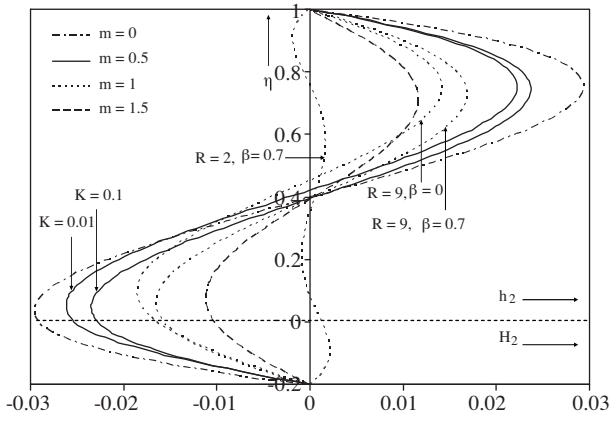

Figure 7. Induced magnetic field h_2, H_2 vs. η for G = 10, K = 0.1, $M^2 = 20$, R = 9, $\beta = 0.7$, $\phi_1 = 1.25$, $\theta = 45$.

Figures 8 and 9 show the rates of heat transfer at the upper impermeable wall for various values of the parameters $R, K, \beta, \phi_1, m, G, \theta$and$M^2$. In these figures the rate of heat transfer is plotted against Brinkman number$NBr(= \Pr Ec)$. It is found that as NBr increases, the rate of heat transfer $\left(\frac{dt}{d\eta}\right)_{\eta=1}$ decreases, and becomes zero for certain Brinkman number (NBr^*), and then changes sign (reversal of the heat flow direction). It is seen from Figures 8 and 9 and the corresponding Tables 1 and 2 that, as the pressure gradient G increases, this reversal of heat flow takes place at smaller NBr, since by increasing G flow is increased in the channel, and so the frictional heat. A similar effect is seen for the parameter β and for the magnetic field M. However, reversal of heat flow takes place at smaller NBr by decreasing the rotation parameter R, or the viscosities ratio ϕ_1, or the parameter K, or the angle of inclination θ, or the Hall current parameter m.

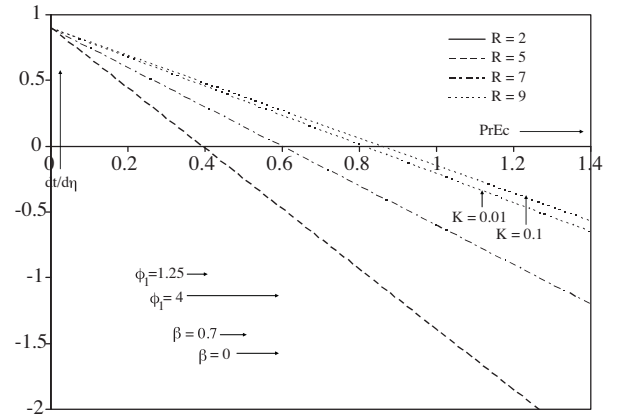

Figure 8. Rate of heat transfer $\left(\frac{dt}{d\eta}\right)_{\eta=1}$ vs. PrEc for G = 10, K = 0.1, m = 1, $M^2 = 20$, $\beta = 0.7$, $\phi_1 = 1.25$, $\phi_2 = 1.67$, $\theta = 45$.

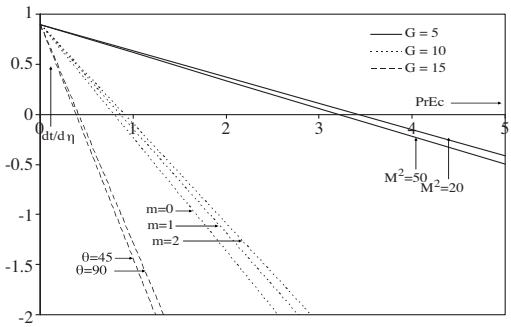

Figure 9. Rate of heat transfer $\left(\frac{dt}{d\eta}\right)_{\eta=1}$ vs. PrEc for K = 0.1, m = 1, $M^2 = 20$, R = 9, $\beta = 0.7$, $\phi_1 = 1.25$, $\phi_2 = 1.67$, $\theta = 45$.

Table 1. Depicting the critical values of NBr at which $\left(\frac{dt}{d\eta}\right)_{\eta=1} = 0$ in Figure 8.

R	$\phi 1$	β	K	NBr*
2	1.25	0.7	0.1	0.192798
2	1.25	0	0.1	0.215634
2	4	0.7	0.1	0.257066
5	1.25	0.7	0.1	0.389834
7	1.25	0.7	0.1	0.596155
9	1.25	0.7	0.01	0.806927
9	1.25	0.7	0.1	0.85521

Table 2. Depicting the critical values of NBr at which $\left(\frac{dt}{d\eta}\right)_{\eta=1} = 0$ in Figure 9.

G	M^2	M	θ	NBr*
15	20	1	45	0.380093
15	20	1	90	0.408414
10	20	0	45	0.787752
10	20	1	45	0.85521
10	20	2	45	0.89847
5	50	1	45	3.210924
5	20	1	45	3.420839

The temperature distribution for various values of the product PrEc is seen plotted in Figures 10 and 11. It is observed that when Pr Ec=0, the temperature distribution is linear. For PrEc> 0, a parabolic distribution is superimposed on it, which is due to the heat generated through viscous and joule dissipation. It is observed that the temperature in the channel increases with increasing PrEc whereas the magnetic field M decreases it. Further, it is seen that the effect of the rotation parameter R is to decrease the temperature in the channel. Because of rotation, it is seen that the rate of heat transfer at the upper plate decreases. Increasing rotation therefore opposes the conduction of heat from the upper plate of the channel into the fluid, causing a decrease in fluid temperature in the channel. Similar results have been reported by Ghosh et al. (2009). Moreover, it is seen that when the Hall parameter m is small, and when it increases from $m = 0$ to $m = 1$, temperature is reduced. Further, it is also reduced when the permeability of the porous substrate attached to the lower wall is increased from $K = 0.01$ to $K = 0.1$.

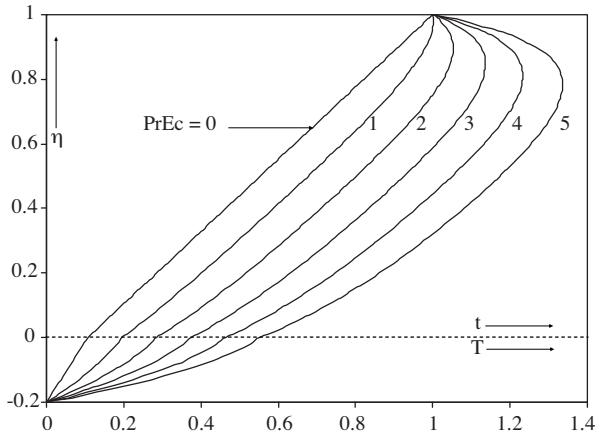

Figure 10. Temperature distribution t, T vs. η for G = 10, K = 0.1, m = 1, $M^2 = 20$, R = 9, $\beta = 0.7$, $\phi_1 = 1.25$, $\phi_2 = 1.67$, $\theta = 45$.

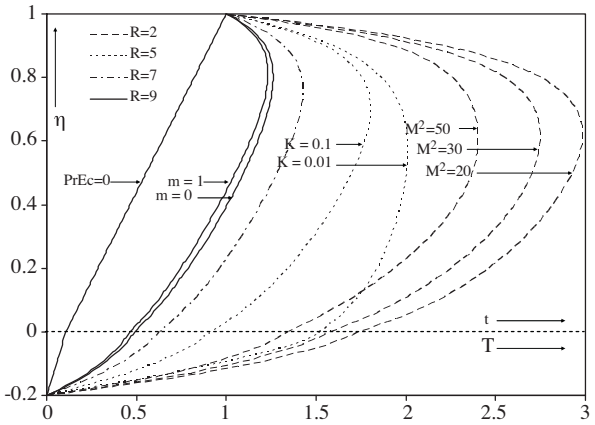

Figure 11. Temperature distribution t, T vs. η for G = 10, K = 0.1, m = 1, $M^2 = 20$, PrEc = 4, $\beta = 0.7$, $\phi_1 = 1.25$, $\phi_2 = 1.67$, $\theta = 45$.

Conclusion

We have investigated the Poiseuille flow of a viscous conducting fluid in a composite parallel plate channel, rotating with a uniform angular velocity about an axis normal to the plates, in the presence of an inclined

magnetic field. The flow is induced by a constant pressure gradient and the fluid and plates rotate in unison with the same constant angular velocity. A porous substrate of finite thickness is attached to the lower plate. Hall current is also taken into account.

The effects of various parameters on the flow and heat transfer are observed from the graphs, and are summarized as follows:

1. The velocity components in the primary flow direction decreases with an increase in R, m, or ϕ_1
2. With an increase in K or β, the primary flow increases in the porous region and near its surface, whereas it decreases in the middle and upper part of the channel.
3. With an increase in K, m, β, or θ, the secondary flow increases, whereas it decreases with an increase in ϕ_1 and becomes oscillatory with an increase in R.
4. The induced magnetic field in the primary flow direction increases with an increase in m, whereas in the secondary flow direction it decreases. However, the effect of R is just reverse to that of m.
5. With an increase in K or β, both induced magnetic fields in primary and secondary flow direction decrease in the porous region and near its surface, whereas both increase in the upper part of the channel.
6. Rate of heat transfer at the upper wall decreases with an increase in NBr, becomes zero at certain Brinkman number (NBr^*), and then changes sign. This change occurs early by decreasing R, K, ϕ_1, θ, or m, or by increasing G, β, or M.
7. Temperature in the channel increases with an increase in Brinkman number NBr(=PrEc), and decreases with an increase in R, m, or K.

Acknowledgement

The authors wish to express their very sincere thanks to the reviewers for their valuable suggestions and comments. The support provided by the University Grants Commission through Junior Research Fellowship to one of the authors, Ms. Priyanka Rastogi, is gratefully acknowledged.

Nomenclature

C_p	specific heat at constant pressure
e	electric charge
Ec	Eckart number
E_1'	induced electric field in clear fluid in x-direction
E_2'	induced electric field in clear fluid in y-direction
E_3'	induced electric field in clear fluid in z-direction
$\bar{E}'_1$	induced electric field in porous medium in x-direction
$\bar{E}'_2$	induced electric field in porous medium in y-direction
$\bar{E}'_3$	induced electric field in porous medium in z-direction
G	non-dimensional pressure gradient
H_0	applied magnetic field
h_1	induced magnetic field in clear fluid in x-direction
h_2	induced magnetic field in clear fluid in y-direction
H_1	induced magnetic field in porous medium in x-direction
H_2	induced magnetic field in porous medium in y-direction
J_1'	current density in clear fluid in x-direction
J_2'	current density in clear fluid in y-direction
$\bar{J}'_1$	current density in porous medium in x-direction
$\bar{J}'_2$	current density in porous medium in y-direction
k	thermal conductivity of clear fluid

$\overline{k}$ effective thermal conductivity of fluid in porous medium
K non-dimensional permeability of porous layer
m Hall current parameter $(= \tau_e \omega_e)$
M Hartmann number
NBr Brinkman number $(= \Pr Ec)$
p_e electron pressure
Pr Prandtl number
R rotation parameter
t temperature in clear fluid region
T temperature in porous region
u velocity in clear fluid in x-direction
v velocity in clear fluid in y-direction
U velocity in porous medium in x-direction
V velocity in porous medium in y-direction

Greek symbols

β adjustable parameter in the jump boundary condition
ϕ_1 viscosities ratio $(= \overline{\mu}/\mu)$
ϕ_2 conductivities ratio $\left(= \overline{k}/k\right)$
η non-dimensional coordinate in the z-direction $(= z/L)$
η_e number density of electron
μ viscosity of the clear fluid
$\overline{\mu}$ effective viscosity of fluid in porous medium
μ_e magnetic permeability
θ angle of inclination of magnetic field
ρ fluid density
σ electrical conductivity
υ kinematic coefficient of viscosity
Ω angular velocity
τ_e electron collision time
ω_e cyclotron frequency

References

Al-Nimr, M.A. and Khadrawi, A.F., "Transient Free Convection Fluid Flow in Domains Partially Filled with Porous Media", Transport in Porous Media, 51, 157-172, 2003.

Armstead, H.C., Geothermal Energy, EN Spon. London, 1982.

Bear, J. and Bachmat, Y., Introduction to Modeling of Ground Water Pollution, Dordrecht, Netherlands, 1987.

Bég, O.A., Takhar H.S., Zueco J., Sajid A. and Bhargava R., "Transient Couette Flow in a Rotating Non-Darcian Porous Medium Parallel Plate Configuration: Network Simulation Method Solutions", Acta. Mech., 200, 129-144, 2008.

Bian, W., Vasseur, P. and Bilgen, E., "Effect of an Electromagnetic Field on Natural Convection in Inclined Porous Layers", Int. J. Heat Fluid Flow, 17, 36-44, 1996.

Chauhan, D. S. and Gupta, S., "Heat Transfer in Couette Flow of a Compressible Newtonian Fluid through a Channel with Highly Permeable Layer at the Bottom". Modelling, Measurement and Simulation B, 67(2), 37-52, 1999.

Chauhan, D. S. and Jain, R., "Three Dimensional MHD Steady Flow of a Viscous Incompressible Fluid Over a Highly Porous Layer", Modelling, Measurement and Control B, 74(5), 19-34, 2005.

Childress, S. and Soward, A.M., "Convection-Driven Hydromagnetic Dynamo", Phys. Rev. Lett, 29, 837, 1972.

Cowling, T.G., Magnetohydrodynamics, New York: Interscience Pub. Inc., 1957.

Eltayeb, I.A., "Hydromagnetic Convection in a Rapidly Rotating Fluid Layer", Proc. R. Soc. Lond. A. 326, 229, 1972.

Eltayeb, I.E. and Roberts, P.H., "On the Hydromagnetics of Rotating Fluids", Astrophys. J., 162, 699, 1970.

Geindreau, C. and Auriault, J.L., "Magnetohydrodynamic Flows in Porous Media", J. Fluid. Mech. 466, 343-363, 2002.

Ghosh, S.K., "Effects of Hall Current on MHD Couette Flow in a Rotating System with Arbitrary Magnetic Field", Czech. J. Phys., 52, 51-63, 2002.

Ghosh, S.K. and Bhattacharjee, P.K., "Hall Effects on Steady Hydromagnetic flow in a Rotating Channel in the Presence of an Inclined Magnetic Field", Czech. J. Phys., 50(6), 759-767, 2000.

Ghosh, S.K., Bég, O.A. and Narahari, M., "Hall Effects on MHD Flow in a Rotating System with Heat Transfer Characteristics", Meccanica, DOI 10.1007/s11012-009-9210-6, Published Online: 2009.

Hayat, T., Husain, M. and Khan, M., "Effects of Hall Current on Flows of a Burger's Fluid through a Porous Medium", Transp. Porous Med., 68, 249-263, 2007a.

Hayat, T., Javed, M. and Ali, N., "MHD Peristaltic Transport of a Jeffery Fluid in a Channel with Compliant Walls and Porous Space", Trans. Porous Media, 74, 259-274, 2008.

Hayat, T., Khan, S.B., Sajid, M. and Asghar, S., "Rotating Flow of a Third Grade Fluid in a Porous Space with Hall Current", Nonlinear Dynamics, 49, 83-91, 2007b.

Hayat, T., Khan, S.B. and Khan, M., "The Influence of Hall Current on the Rotating Oscillating flows of an Oldroyd-B Fluid in a Porous Medium", Nonlinear Dynamics, 47, 353-362, 2007c.

Hayat, T., Nadeem, S., Asghar, S. and Siddiqui, A.M., "Effects of Hall Current on Unsteady flow of a Second Grade Fluid in a Rotating System", Chemical Engng. Comm., 192, 1272-1284, 2005.

Kim, S. and Russell, W.B., "Modeling of Porous Media by Renormalization of the Stokes Equation", J. Fluid Mech., 154, 269-286, 1985.

Krishna, D.V., Prasada Rao, D.R.V. and Ramachandra Murthy, A.S., "Hydromagnetic Convection Flow Through a Porous Medium in a Rotating Channel", J. of Engng. Phys. and Thermophysics, 75(2), 281-291, 2002.

Kuznetsov, A.V., "Analytical Investigation of the Fluid Flow in the Interface Region between a Porous Medium and a Clear Fluid in Channels Partially Filled with a Porous Medium", Appl. Sci. Res., 56, 53-57, 1996.

Kuznetsov, A.V., "Analytical Investigation of Couette Flow in a Composite Channel Partially Filled with a Porous Medium and Partially with a Clear Fluid", Int. J. Heat Mass Transfer, 41(16), 2556-2560, 1998.

Kuznetsov, A.V., "Fluid Flow and Heat Transfer Analysis of Couette Flow in a Composite Duct", Acta Mechnica, 140, 163-170, 2000.

Mandal, G. and Mandal, K.K., "Effect of Hall Current on MHD Couette Flow between Thick Arbitrarily Conducting Plates in a Rotating System", J. Physical Soc. Japan, 52, 470-477, 1983.

McWhirter, J., Crawford, M., Klein, D. and Sanders, T., "Model for Inertia Less Magnetohydrodynamic Flow in Packed Beds", Fusion Technol., 33, 22-30, 1998a.

McWhirter, J., Crawford, M. and Klein, D., "Magnetohydrodynamic flows in Porous Media II: Experimental Results, Fusion Technol", 34, 187-197, 1998b.

Nield, D.A., "Modeling the Effects of a Magnetic Field or Rotation on Flow in a Porous Medium. Momentum Equation and Anisotropic Permeability Analogy", Int. J. Heat Mass Transfer, 42, 3715-3718, 1999.

Nield, D.A. and Bejan, A., Convection in Porous Media, Springer, USA, 2006.

Ochao-Tapia, J.A. and Whitaker, S., "Momentum Transfer at the Boundary between a Porous Medium and a Homogeneous Fluid-I. Theoretical Development." Int. J. Heat Mass Transfer, 38 (14): 2635-2646, 1995a.

Ochao-Tapia, J.A. and Whitaker, S., "Momentum Transfer at the Boundary between a Porous Medium and a Homogeneous Fluid-I. Comparison with Experiment." Int. J. Heat Mass Transfer, 38 (14): 2647-2655, 1995b.

Raghavachar, M.R. and Gothandaraman, V.S., "Hydromagnetic Convection in a Rotating Fluid Layer in the Presence of Hall Current", Geophysical and Astrophysical Fluid Dynamics, 45 (3), 199-211, 1989.

Riahi, D.N., "Effects of Rotation on Convection in a Porous Layer during Alloy Solidification". In Transport Phenomena in Porous Media II: eds: D.B. Ingham and I. Pop, Pergamon, Oxford, UK, 316-340, 2002.

Seddeek, M.A., "Effects of Magnetic Field and Variable Viscosity on Forced Non-Darcy Flow about a Flat Plate with Variable Wall Temperature in Porous Media in the Presence of Suction and Blowing", J. Appl. Mech. and Tech. Phys. 43 (1), 13-17, 2002.

Seth, G.S., Nandkeolyar, R. and Mahto, N., "MHD Couette Flow in a Rotating System in the Presence of an Inclined Magnetic Field", Appl. Mathematical Sciences, 3(59), 2919-2932, 2009.

Singh, A.K., Sacheti, N.C. and Chandran, P., "Transient Effects in Magneto-Hydrodynamic Couette Flow with Rotation: Accelerated Motion", Int. J. Engng. Sci., 32, 133-139, 1994.

Sunil and Mahajan, A., "A Nonlinear Stability Analysis for Rotating Magnetized Ferrofluid Heated from Below Saturating a Porous Medium", Z. Angew. Math. Phys. 60, 344-362, 2009.

Sutton, G.W. and Sherman, A., Engineering Magnetohydrodynamics, McGraw-Hill, N.Y., 1965.

Appendix

$$A^2 = \left(\frac{M^2\cos^2\theta}{1+m^2\cos^2\theta}\right) + i\left(2R + \frac{M^2 m\cos^3\theta}{1+m^2\cos^2\theta}\right) = a_1 + ia_2,$$

$$A = \left(\frac{\sqrt{a_1^2+a_2^2}+a_1}{2}\right)^{1/2} + i\left(\frac{\sqrt{a_1^2+a_2^2}-a_1}{2}\right)^{1/2} = a_3 + ia_4,$$

$$B = \left(\frac{M^2\cos\theta}{1+m^2\cos^2\theta}\right) + i\left(\frac{M^2 m\cos^2\theta}{1+m^2\cos^2\theta}\right) = b_1 + ib_2,$$

$$C^2 = \left(\frac{a_1}{\phi_1} + K_1\right) + i\left(\frac{a_2}{\phi_1}\right) = c_1 + ic_2,$$

$$C = \left(\frac{\sqrt{c_1^2+c_2^2}+c_1}{2}\right)^{1/2} + i\left(\frac{\sqrt{c_1^2+c_2^2}-c_1}{2}\right)^{1/2} = c_3 + ic_4,$$

$$D = \left(\frac{1}{1+m^2\cos^2\theta}\right) + i\left(\frac{m\cos\theta}{1+m^2\cos^2\theta}\right) = d_0 + id_0',$$

$$D_1 = \sinh A, \quad D_2 = \cosh A, \quad D_3 = \sinh C\alpha, \quad D_4 = \cosh C\alpha,$$

$$P_1 = \frac{B^2}{M^2}\left[\frac{1}{A^2} + \frac{\alpha}{\phi_1 C^2} + \frac{D_3}{CA^2} - \frac{D_3}{\phi_1 C^3} + \frac{\beta}{\sqrt{K}}\frac{(1-D_4)}{\phi_1 C^2 A^2}\right] - D(1+\alpha),$$

$$P_2 = \frac{B^2}{M^2}\left[\frac{D_2-1}{A} + \frac{(1-D_4)A}{\phi_1 C^2}\right], \quad P_3 = \frac{B^2}{M^2}\left[\frac{D_1}{A} + \frac{D_3}{C} + \frac{\beta}{\sqrt{K}}\frac{(1-D_4)}{\phi_1 C^2}\right],$$

$$P_4 = \frac{1}{\phi_1 C^2} + \frac{D_4}{A^2} - \frac{D_4}{\phi_1 C^2} - \frac{\beta}{\sqrt{K}}\frac{D_3}{\phi_1 C A^2}, \quad P_5 = -\frac{AD_3}{\phi_1 C}, \quad P_6 = D_4 - \frac{\beta}{\sqrt{K}}\frac{D_3}{\phi_1 C},$$

$$P_7 = P_2 - A^2 D_1 P_1, \quad P_8 = P_3 - A^2 D_2 P_1, \quad P_9 = P_5 - A^2 D_1 P_4, \quad P_{10} = P_6 - A^2 D_2 P_4,$$

$$A_2 = -\frac{GD(1+\alpha)P_{10}}{P_7 P_{10} - P_9 P_8}, \quad A_3 = -\frac{P_9}{P_{10}}A_2, \quad B_2 = \frac{1}{\phi_1 C}\left[A_2\left(A - \frac{\beta}{\sqrt{K}}D_1\right) + \frac{\beta}{\sqrt{K}}A_3(1-D_2)\right],$$

$$B_3 = A_3\left(1 - D_2 + \frac{A^2 D_2}{\phi_1 C^2}\right) - A_2 D_1\left(1 - \frac{A^2}{\phi_1 C^2}\right),$$

$$A_1 = -\frac{1}{D\,(1+\alpha)}\frac{B}{M^2}\left[A_2\left(\frac{D_2-1}{A} - D_1 - \frac{\alpha A^2 D_1}{\phi_1 C^2}\right) + A_3\left(\frac{D_1}{A} - D_2 - \frac{\alpha A^2 D_2}{\phi_1 C^2}\right) + B_2\left(\frac{1-D_4}{C}\right) + B_3\left(\frac{D_3}{C}\right)\right],$$

$$B_1 = A_1, \quad A_4 = -\left[A_1 D + \frac{B}{M^2}\left(\frac{G - BA_1}{A^2} + \frac{A_2 D_2 + A_3 D_1}{A}\right)\right],$$

$$B_4 = A_1 D\alpha + \frac{B}{M^2}\left[\left(\frac{G - BA_1}{\phi_1 C^2}\right)\alpha - \left(\frac{B_2 D_4 - B_3 D_3}{C}\right)\right],$$

$$Q_6 = \frac{G - BA_1}{A^2}, \quad Q_7 = \frac{G - BA_1}{\phi_1 C^2}, \quad Q_{15} = A_1 D, \quad Q_{16} = BQ_{15}^c,$$

$$F_1 = \frac{1}{2}\left(a_{21}^2 + a_{22}^2 + a_{31}^2 + a_{32}^2\right)\left(a_3^2 + a_4^2 + \frac{b_1^2 + b_2^2}{M^2}\right),$$

$$F_2 = \frac{1}{2}\left(a_{21}^2 + a_{22}^2 - a_{31}^2 - a_{32}^2\right)\left(a_3^2 + a_4^2 - \frac{b_1^2 + b_2^2}{M^2}\right),$$

$$F_3 = 2\left[\left(\frac{b_1^2 + b_2^2}{M^2}\right)(a_{21}q_{11} + a_{22}q_{12}) + (a_{21}q_{31} - a_{22}q_{32})\right],$$

$$F_4 = -2\left[\left(\frac{b_1^2 + b_2^2}{M^2}\right)(a_{22}q_{11} - a_{21}q_{12}) + (a_{22}q_{31} + a_{21}q_{32})\right],$$

$$F_5 = 2\left[\left(\frac{b_1^2 + b_2^2}{M^2}\right)(a_{31}q_{11} + a_{32}q_{12}) + (a_{31}q_{31} - a_{32}q_{32})\right],$$

$$F_6 = -2\left[\left(\frac{b_1^2 + b_2^2}{M^2}\right)(a_{32}q_{11} - a_{31}q_{12}) + (a_{32}q_{31} + a_{31}q_{32})\right],$$

$$F_7 = (a_{21}a_{31} + a_{22}a_{32})\left(a_3^2 + a_4^2 + \frac{b_1^2 + b_2^2}{M^2}\right), \quad F_8 = (a_{22}a_{31} - a_{21}a_{32})\left(a_3^2 + a_4^2 - \frac{b_1^2 + b_2^2}{M^2}\right),$$

$$F_9 = \left[M^2\left(q_{29}^2 + q_{30}^2\right) + \left(\frac{b_1^2 + b_2^2}{M^2}\right)\left(q_{11}^2 + q_{12}^2\right) + 2\left(q_{11}q_{31} - q_{12}q_{32}\right)\right],$$

$$F_{10} = \frac{a_3 F_5 - a_4 F_6}{a_3^2 + a_4^2}, \quad F_{11} = \frac{a_4 F_5 + a_3 F_6}{a_3^2 + a_4^2}, \quad F_{12} = \frac{a_3 F_3 - a_4 F_4}{a_3^2 + a_4^2}, \quad F_{13} = \frac{a_4 F_3 + a_3 F_4}{a_3^2 + a_4^2},$$

$$F_{14} = \frac{a_3 F_{12} - a_4 F_{13}}{a_3^2 + a_4^2}, \quad F_{15} = \frac{a_4 F_{12} + a_3 F_{13}}{a_3^2 + a_4^2}, \quad F_{16} = \frac{a_3 F_{10} - a_4 F_{11}}{a_3^2 + a_4^2}, \quad F_{17} = \frac{a_4 F_{10} + a_3 F_{11}}{a_3^2 + a_4^2},$$

$$F_{18} = \frac{1}{2\phi_2}\left(b_{21}^2 + b_{22}^2 + b_{31}^2 + b_{32}^2\right)\left[\frac{1}{K} + \phi_1\left(c_3^2 + c_4^2\right) + \frac{b_1^2 + b_2^2}{M^2}\right],$$

$$F_{19} = \frac{1}{2\phi_2}\left(-b_{21}^2 - b_{22}^2 + b_{31}^2 + b_{32}^2\right)\left[\frac{1}{K} - \phi_1\left(c_3^2 + c_4^2\right) + \frac{b_1^2 + b_2^2}{M^2}\right],$$

$$F_{20} = \frac{2}{\phi_2}\left[\left(\frac{1}{K} + \frac{b_1^2 + b_2^2}{M^2}\right)(b_{21}q_{13} + b_{22}q_{14}) + (b_{21}q_{31} - b_{22}q_{32})\right],$$

$$F_{21} = -\frac{2}{\phi_2}\left[\left(\frac{1}{K}+\frac{b_1^2+b_2^2}{M^2}\right)(b_{22}q_{13}-b_{21}q_{14})+(b_{22}q_{31}+b_{21}q_{32})\right],$$

$$F_{22} = \frac{2}{\phi_2}\left[\left(\frac{1}{K}+\frac{b_1^2+b_2^2}{M^2}\right)(b_{31}q_{13}+b_{32}q_{14})+(b_{31}q_{31}-b_{32}q_{32})\right],$$

$$F_{23} = -\frac{2}{\phi_2}\left[\left(\frac{1}{K}+\frac{b_1^2+b_2^2}{M^2}\right)(b_{32}q_{13}-b_{31}q_{14})+(b_{32}q_{31}+b_{31}q_{32})\right],$$

$$F_{24} = \frac{1}{\phi_2}(b_{21}b_{31}+b_{22}b_{32})\left[\frac{1}{K}+\phi_1\left(c_3^2+c_4^2\right)+\frac{b_1^2+b_2^2}{M^2}\right],$$

$$F_{25} = -\frac{1}{\phi_2}(b_{22}b_{31}-b_{21}b_{32})\left[\frac{1}{K}-\phi_1\left(c_3^2+c_4^2\right)+\frac{b_1^2+b_2^2}{M^2}\right],$$

$$F_{26} = \frac{1}{\phi_2}\left[M^2\left(q_{29}^2+q_{30}^2\right)+\left(\frac{1}{K}+\frac{b_1^2+b_2^2}{M^2}\right)\left(q_{13}^2+q_{14}^2\right)+2\left(q_{13}q_{31}-q_{14}q_{32}\right)\right],$$

$$F_{27} = \frac{c_3F_{22}-c_4F_{23}}{c_3^2+c_4^2},\quad F_{28} = \frac{c_4F_{22}+c_3F_{23}}{c_3^2+c_4^2},\quad F_{29} = \frac{c_3F_{20}-c_4F_{21}}{c_3^2+c_4^2},\quad F_{30} = \frac{c_4F_{20}+c_3F_{21}}{c_3^2+c_4^2},$$

$$F_{31} = \frac{c_3F_{29}-c_4F_{30}}{c_3^2+c_4^2},\quad F_{32} = \frac{c_4F_{29}+c_3F_{30}}{c_3^2+c_4^2},\quad F_{33} = \frac{c_3F_{27}-c_4F_{28}}{c_3^2+c_4^2},\quad F_{34} = \frac{c_4F_{27}+c_3F_{28}}{c_3^2+c_4^2},$$

$$F_{35} = \tfrac{F_1}{4a_3^2}\cosh 2a_3 - \tfrac{F_2}{4a_4^2}\cos 2a_4 + \tfrac{F_7}{4a_3^2}\sinh 2a_3 - \tfrac{F_8}{4a_4^2}\sin 2a_4 + F_{14}\sinh a_3\cos a_4 + F_{15}\cosh a_3\sin a_4 + F_{16}\cosh a_3\cos a_4 + F_{17}\sinh a_3\sin a_4 + \tfrac{F_9}{2}$$

$$F_{36} = \frac{F_1}{4a_3^2}-\frac{F_2}{4a_4^2}+F_{16}-\frac{F_{18}}{4c_3^2}+\frac{F_{19}}{4c_4^2}-F_{33},\quad F_{37} = \left(\frac{F_7}{2a_3}-\frac{F_8}{2a_4}+F_{12}\right)-\phi_2\left(\frac{F_{24}}{2c_3}-\frac{F_{25}}{2c_4}+F_{29}\right),$$

$$F_{38} = \frac{F_{18}}{4c_3^2}\cosh 2c_3\alpha - \frac{F_{19}}{4c_4^2}\cos 2c_4\alpha - \frac{F_{24}}{4c_3^2}\sinh 2c_3\alpha + \frac{F_{25}}{4c_4^2}\sin 2c_4\alpha - F_{31}\sinh c_3\alpha\cos c_4\alpha - F_{32}\cosh c_3\alpha\sin c_4\alpha + F_{33}\cosh c_3\alpha\cos c_4\alpha + F_{34}\sinh c_3\alpha\sin c_4\alpha + \frac{F_{26}}{2}\alpha^2,$$

$$F_{39} = \frac{F_{36}+F_{37}+F_{38}-F_{35}}{\alpha+\phi_2},\quad E_3 = \Pr Ec\ F_{39}-\frac{1}{\alpha+\phi_2},\quad E_4 = \Pr Ec\ (\alpha F_{39}-F_{38})-\frac{\alpha}{\alpha+\phi_2},$$

$E_1 = \Pr Ec\ (\phi_2F_{39}-F_{37})-\frac{\phi_2}{\alpha+\phi_2}$, $E_2 = \Pr Ec\ (\alpha F_{39}-F_{38}-F_{36})-\frac{\alpha}{\alpha+\phi_2}$ a_{21}, a_{31}, b_{21}, b_{31}, q_{11}, q_{13}, q_{29}, q_{31} are the real parts of $A_2, A_3, B_2, B_3, Q_6, Q_7, Q_{15}, Q_{16}$ respectively and a_{22}, a_{32}, b_{22}, b_{32}, q_{12}, q_{14}, q_{30}, q_{32} are the imaginary parts of $A_2, A_3, B_2, B_3, Q_6, Q_7, Q_{15}, Q_{16}$ respectively.